Research paper

Methodology for optimizing a Constellation of a Lunar Global Navigation System with a multi-objective optimization algorithm

Angel David Arcia Gil [a,*], Daniel Renwick [b], Chantal Cappelletti [b], Paul Blunt [c]

[a] School of Telecommunications, Doctoral Programme in Aerospace Technology: Electromagnetic, Electronic, Computer and Mechanical Engineering, University of Vigo, Spain
[b] Department of Mechanical, Materials and Manufacturing Engineering, University of Nottingham, UK
[c] Nottingham Geospatial Institute, University of Nottingham, UK

ARTICLE INFO

ABSTRACT

Global Navigation Satellite Systems (GNSS) are not only used in terrestrial applications, but also in Low-Earth orbit satellites and in higher altitude missions. NASA's Magnetospheric Multiscale (MMS) mission has demonstrated the capabilities of existing GNSS systems to provide positioning, navigation, and timing (PNT) services in the Cis-lunar space.

The resurgence in plans by national space agencies for Lunar exploration presents a need for accurate, precise, and reliable navigation systems to ensure the safety and success of future missions.

Moreover, the increased amount of Moon missions over recent years, shows the requirement of navigation capabilities for Low Lunar orbiters, Moon landers, Moon rovers, and manned missions.

The success of Global Navigation Satellite Systems (GNSS) on Earth, presents an opportunity for the study of a potential design requirements and expected performance of a Lunar GNSS constellation.

We have approached this problem through the methodology of multi-objective optimization; numerically simulating the orbits, and using the Position Dilution of Precision (PDoP) as the figure of merit to optimize a set of 200 constellation designs and improving them gradually over 1864 generations. Over 12,000 unique constellation designs were generated with the best 10 constellations presented in this paper for consideration and further study. Compared to the literature, these 10 constellations achieved a 44% improvement in PDoP (2.73) using the same number of satellites in each constellation, and meeting the performance requirements of planned Lunar missions.

1. Introduction

With a resurgence in institutional desire to conduct human space exploration, the Moon is considered an important milestone to assess new technologies in the preparation for crewed Martian expeditions. NASA's Artemis program, aiming to return humans to the Moon by the end of the decade, will be the first of these, and has the goal to create the first permanent human presence on the Moon. Alongside these crewed missions will be the need of autonomous spacecraft in support roles, such as cargo missions, exploratory rovers, and robotic resource prospecting missions [1–4].

The success and safety of these missions will depend on the ability to accurately calculate the spacecraft or astronauts' position, velocity and timing during all stages of the journey.

Previous research [5–8] has considered the use of existing GNSS constellations for navigation in Lunar transfer trajectories and in Lunar orbit. In Lunar transfer trajectories, GNSS Positioning, Navigation and Timing (PNT) calculations can be performed with 98.8% availability, however once in Lunar orbit, the availability drops to 11.6% [5]. 11.6% availability would be sufficient for periodic Lunar navigation, however for continuous PNT determination, a dedicated Lunar GNSS constellation would be required.

Research conducted in [9] investigates the use of GNSS signals for navigation not limited to only Lunar transfer and Lunar orbits, but also adding analysis of ascent/descent phases, surface operations, and L1/L2 Lagrange points.

The aim of this paper, therefore, is to design and analyze the performance of a Lunar GNSS constellation and is the natural progression of the European Space Agency's (ESA) NaviMoon Project [10], which aims to assess the feasibility of an Earth–Moon Navigation System, and the development of a highly-sensitive spaceborne receiver prototype. There has been previous research into the design of a Lunar GNSS constellation, with provisional constellation designs proposed [11,12].

Research in the literature has been limited to either being a purely analytical study [11] or by restricting the range of orbits considered in a numerical simulation to frozen orbit conditions, having an orbital inclination restricted to 40° [12] We will build on this work by numerically analyzing a greater range of orbital arrangements and by comparing the performance of each against the PNT requirements of proposed Lunar missions [10].

2. Background review

Before designing a novel GNSS constellation for future Lunar missions, it is crucial to understand the theory of satellite constellation design and the metrics by which to measure their performance for GNSS navigation. The key-concepts utilized in this paper are briefly explained in this section.

2.1. Principle of GNSS

A GNSS constellation is made up of a system of satellites, each of which transmit ranging codes and navigation data, allowing a receiver to determine the transmission time and current location of the transmitting satellite. GNSS makes use of time-of-arrival (TOA) ranging by comparing the times of transmission and arrival and relative position, from at least four satellites in orbit, allowing the receiving device to calculate its three-dimensional position, velocity and timing (PVT) [13].

2.2. Satellite constellation design

In designing a satellite constellation, one is optimizing particular orbital parameters with the aim of producing a constellation meeting the desired performance requirements at a minimum cost. One of the key parameters to optimize is the number of satellites and the number of planes on which they orbit.

A constellation intended to observe a single location has different requirements to one which intends global coverage, and in the case of this paper, we have used the latter, by using Walker [14], and Rider [15] methodologies.

The Rider method constructs the constellations from groups of satellites on inclined circular orbits, each of the same altitude and inclination. These constellations are limited to those with equal phasing between planes, which are also equally spaced [15]. Rider computed a number of tables detailing optimal configurations of P, S, and c, for various orbital inclination and Earth coverage (global, regional, etc.), where P is defined as the number of orbital planes, S is the number of satellites per plane, and c is the half street width [13]. These tables can then be used to compare a number of possible solutions for a use-case (i.e., P:3, S:4 vs P:2, S:5).

Like Rider constellations, Walker constellations use inclined circular orbits, each with the same altitude and inclination, however Walker constellation allow for a more generalized definition as they allow for unequal phasing between orbital planes. Walker constellations are defined by a given orbital inclination, i, and by the T/P/F notation; where T is the total number of satellites, P is the number of orbital planes, and F is the phase offset between adjacent orbital planes. If S is defined as the number of satellites per plane, then T is equal to P multiplied by S as in Rider constellations. F is defined as an integer such that $0 \leq F \leq P - 1$, and the offset in mean anomaly between the first satellite in each adjacent plane is $\frac{2\pi F}{P}$ [13].

The importance of redundancy has to be considered in both Rider and Walker models. Since Navigation constellations are constrained to provide multiple coverage, the design is focused on the minimum number of platforms.

Walker's results with respect to streets of coverage model by Rider, and also explored by Beste in [16] leads to prefer the first one, although the approaches by their own cannot take into account the robustness to failures from the beginning.

Table 1
Typical contributions to UERE on Earth [13].

Source of error	1σ Range error (m)
Broadcast Clock	1.1
Broadcast Ephemeris	0.8
Receiver Noise and Resolution	0.1
Multipath Error	0.2

2.3. Dilution of precision

The key metric used to determine the performance of a GNSS constellation is the dilution of precision (DoP). DoP is a non-dimensional value indicating the uncertainty in positional measurement due to the relative spacing of the GNSS satellites in view of the receiver [17].

When the transmitted signals originate from spatially distributed points, relative to the observer's point of view, the resultant error from the signal's uncertainty is minimized. However, when the signal sources are close together, relative to the observer, the calculation uncertainty increases. A higher value of DoP represents greater uncertainty in the measurement.

2.4. User equivalent range error

To convert the non-dimensional DoP values into actual measurement uncertainty, the product of the DoP and User Equivalent Range Error (UERE) is taken. The UERE is the total numerical error as a result of the uncertainties arising due to error in each stage of transmission/reception process [13], due to the hardware and environment of the GNSS system. Sources of error can include time error in the satellites' atomic clock and current position, atmospheric effects, and errors arising in the GNSS receiver on the user. To calculate the total UERE of the system, the error values are root-sum-squared [13]. If the error in each value is calculated to 3σ, then the error in the value of the total UERE is also to 3σ.

To convert the navigation requirements of Lunar missions into DoP equivalent values, a representative value of the UERE must be chosen. For this paper we have used the average values of a receiver on the Earth, negating errors due to atmospheric effects, which are listed in Table 1.

Taking the root-sum-square of these four values results in an assumed UERE of 1.4 m as seen in Eq. (1).

$$UERE, \sigma_R = \sqrt{1.1^2 + 0.8^2 + 0.1^2 + 0.2^2} = 1.4 \ m \qquad (1)$$

3. Lunar navigation requirements

As part of the NaviMoon project coordinated by ESA [10], the University of Nottingham consolidated the position, navigation and timing (PNT) requirements of future lunar missions by performing industry surveys, and contacting experts from space agencies, universities and privates companies. The mission profiles (i.e., the mission goals, orbit parameters and navigation requirements) were also analyzed.

Since this information-gathering strategy relied largely on mission PIs and institution being willing to share data, some of which may be sensitive, a literature review of past, current and future Moon missions was performed in parallel to correlate the information obtained with the data provided by the PIs of the missions contacted, as shown in Fig. 1.

Prior to contact being made, a list of known present and future Moon missions to 2030 was compiled along with a key-information table, as shown in Table 2.

The key information table was sent to the related contacts of 60 missions analyzed, with a response rate of 42% (25 missions), although only 7% provided relevant PNT information. The PNT and orbit information for other missions were found in the literature review.
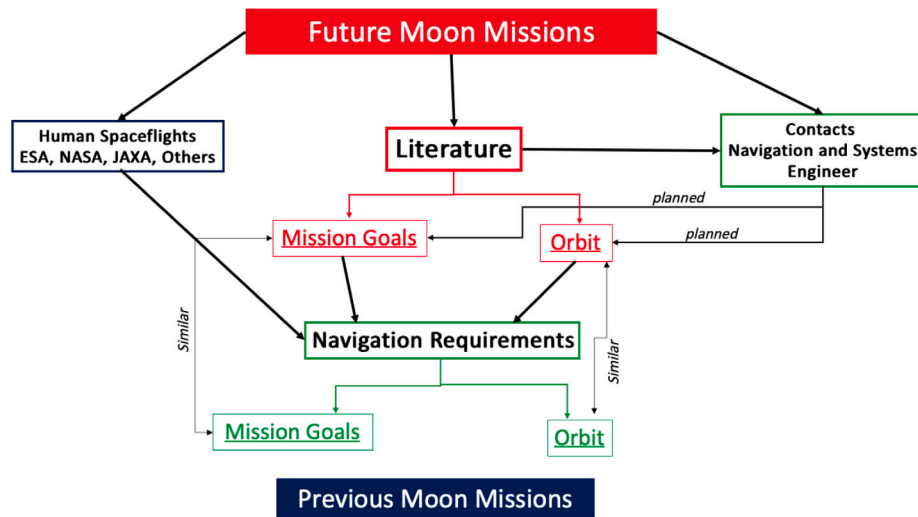
Fig. 1. PNT Information gathering strategy — NaviMoon Project [10].

Table 2
Key-requirements and key-information table [10].

Phase	MTO	Lunar Orbit	Descent and landing	Lunar surface
Key-requirements				
Position requirements (3σ), (m)		Along-Track= Cross-Track= Radial= 3D norm=	Horizontal= Altitude= 3D norm=	Horizontal= X X
Velocity requirements (3σ), (m/s)		Along-Track= Cross-Track= Radial= 3D norm=	Horizontal= Altitude= 3D norm=	Horizontal= X X
Absolutely time accuracy (3σ), (ns)	=	=	=	=
Key-Information				
Orbital Parameters/ Trajectory	=	=	=	=
Attitude pointing mode/s	=	=	=	=

Different mission of the same program such as Artemis 1 – 2 (NASA), Chang'e 5-6-7-8 (CNSA), Luna 25-26-27-28-29 (ROSCOSMOS) among others, were counted as separated missions for the purpose of this study, since the mission goals/type would generate different PNT requirements.

3.1. PNT associated requirements of selected Moon missions

A reduced list of missions was created, as shown in Table 3, based on the relevance related to navigation requirements, parameters found in the literature review and responses to the request for information table received by mission's PIs. The data was used for a critical analysis of the PNT requirements.

3.1.1. Artemis

Even though the specific PNT requirements of Artemis I and Artemis II were not obtained from NASA in the request for information form, the orbital parameters/trajectory found in [18–20] are of importance for the analysis performed in this paper.

Table 3
Reduced list of Moon missions with associated PNT requirements [10].

Mission name	Institution	Type
Artemis I Artemis II	NASA	Flyby
ArgoMoon[a]	Argotec/ASI	Flyby
IM-1	Intuitive Machines	Lander
KPLO	KARI	Orbiter
Lumio	Politecnico Di Milano	Orbiter
Lunar IceCube[a]	Morehead State University	Orbiter
OMOTENASHI[a]	JAXA/University of Tokyo	Lander
Team Indus	Axiom Research Labs	Lander/Rover
Chang'E series	CNSA	Orbiter/Lander/Rover

[a]Secondary payload in the NASA Artemis I flight.

3.1.2. ArgoMoon

Even though the specific PNT requirements of ArgoMoon were not shared by Argotec/ASI, the orbital parameters/trajectory found in the literature [21] are of importance for the analysis performed in this paper.

3.1.3. IM-1

Key-information found in [22], and the key-requirement table provided by Intuitive Machines were analyzed in this study. Intuitive Machines typically defines navigation requirements in relationship to maneuver events rather than as continuous time performance, so some translation may be involved. These are more guidelines than "requirements" and since the system relies on 2-way ranging, there is no strong timing requirement.

3.1.4. KPLO

Key-information found in [23,24], and the key-requirements table provided by the Korean Aerospace Research Institute (KARI) were analyzed in this study.

3.1.5. Lumio

Lumio's concept of operations, orbit, and mission phases can be found in [25,26], and the navigation requirements have been derived through mission analysis in [27].

These requirements conform well with the analysis of [26] which performs Monte-Carlo analysis on station keeping for the orbit considering orbit insertion and determination errors of 10 km (1σ) and 10 cm/s (1σ).

3.1.6. Lunar IceCube

Sample transfer trajectories determined using operational-level software can be found in [28]. From [29], the orbit knowledge of the satellite is stated as: position 10 m, and velocity 0.15 m/s. However, we have no indication on how these are derived or whether they are RMS or 3σ values.

3.1.7. OMOTENASHI

OMOTENASHI utilizes a unique approach for lunar landing by combining the maneuvers for the lunar orbit insertion, descent, and landing into a single maneuver executed by a solid rocket motor, followed by a free-fall onto the lunar surface with impact speed on the order of 30 m/s.

A detailed analysis of the trajectory and the landing phase is performed in [30] where the results suggests accuracy requirements for the landing devices, solid rocket motor and attitude accuracy, as well as to the transfer phase trajectory design.

The results of [30] show a vertical 3σ error of the order of 50 m which will not jeopardize the landing maneuver. The normal landing velocity 3σ variation (m/s) and ground-tangent landing velocity 3σ variation (m/s) are shown in [30].

The key-information and requirements table were provided by JAXA and analyzed in this study.

3.1.8. Team Indus

The key-information and requirements table were provided by Axiom Research Labs and analyzed in this study.

3.1.9. Chang'E series

The "Chang'E" (CE) series missions is an outcome of the China Lunar Exploration Program (CLEP). Started from 2004, the early half of this program consists of three phases — orbiting, landing, and returning. It has completed 5 missions, from CE-1 to CE-4 plus a sub-mission CE-5T. In the latter half of this program, the follow-up missions CE-6 to CE-8 and possible further robotic and manned missions have been planned up to 2030, aiming at 'surveying, constructing, and exploiting' the Moon. The program strategy is shown in [31]. The mission profile of Chang'E-4 can be found in [32].

Although we do not have specific navigation requirements from the Chang'E series, a number of the performance studies were analyzed for achievable performance and the technologies utilized.

After a detailed analysis of missions' navigation requirements, the DoP was calculated by mission type (Table 4), and presented as part of the NaviMoon project review to ESA [10].

As these requirements differ depending on the mission type and location of the receiver, a representative sample of locations must be considered. The GNSS constellations considered will be analyzed based on the DoP performance across the surface of the Moon. With the UERE assumed in this paper, the navigation requirements for the Final Descent Phase during landing and the Moving Phase on the surface are not possible as the minimum DoP possible is 1.0 – the geometry cannot reduce the inherent error in the hardware. For these two requirements, GNSS can be supplemented using on-board navigation methods.

3.2. Proposed Lunar GNSS designs

To study the design of a Lunar GNSS constellation, we have used two papers to draw comparison against: one analyzed the performance of Rider constellations to determine the minimum number of satellites required for full Lunar coverage [11], and the other studied the performance of Walker constellation configurations to determine DoP availability across 500 points on the surface of the Moon [12].

Batista's study [11] proposed a Rider constellation of 30 satellites split over 2 orbital planes at a semi-major axis of 33,400 km. This study is brief and does not specify an orbital inclination for the constellation, nor does it consider the DoP performance of the constellation. Pereira's study [12] proposed a number of optimal solutions with configurations ranging between:

- 5702.3–8916.6 km semi-major axis
- 20–24 satellites
- 3–4 orbital planes
- 40° ±0.5° orbital inclination
- Mean station-keeping ΔV of 0.41 km/s per year

These Walker constellations achieved 95% minimum DoP values between 4.42 and 5.29, almost three times the mean value achieved with existing GNSS constellation on the Earth [17], suggesting that better DoP performance can be achieved with a study that considers a wider range of Walker configurations. The key limitation with Pereira's study is that the orbital inclination of these constellations were limited to 40° delivering poor performance at the poles [12], driving down the mean DoP over the surface.

Other studies such as the one performed in [33] numerically examined the stability of orbits of a Lunar GNSS system, while [34] investigates the design of low and medium frozen orbits considering stability, Moon's surface coverage and revisit times for specific lunar sites, with an optimization algorithm that can be used to draw a comparison with the methodology used in this paper, and explained in the next section.

4. Methodology

To approach the problem of optimizing the design of a GNSS constellation, it must first be abstracted into a function of seven input variables, representing the design of the constellation, and four output objectives, representing the performance metrics of the design as seen in Eq. (2).

$$[PDoP, HDoP, \Delta V, T] = F(a, e, i, \omega, s, p, f) \tag{2}$$

The input variables to optimize are:

- a, semi-major axis, km
- e, eccentricity
- i, inclination, degrees
- ω, argument of periapsis, degrees
- s, number of satellites per plane

Table 4
DoP of future Lunar missions [10].

Mission type/Phase	Measurement type	Desired reliability	DoP metric	DoP equivalent
Descent and Landing				
Initial State	3D Pos.	RMS	PDoP	214
Breaking Phase	3D Pos.	3σ	PDoP	143
Approach Phase	3D Pos.	3σ	PDoP	14
Final Descent Phase	3D Pos.	3σ	PDoP	0.4
Final Landing Location	Hor. Pos.	3σ	HDoP	64
Ascent				
Robotic Mission	3D Pos.	3σ	PDoP	857
Manned Mission	3D Pos.	3σ	PDoP	71
Surface				
Stationary User	3D Pos.	3σ	HDoP	36
Moving Phase	3D Pos.	3σ	HDoP	0.1

- p, number of orbital planes
- f, phase offset of each plane

The output objectives to minimize are:

- PDoP, position dilution of precision
- HDoP, horizontal dilution of precision
- ΔV, change in velocity required for station-keeping, km/s
- T, total number of satellites in the constellation

We can then separate the methodology into two sections: the setup used to simulate the performance of each constellation and retrieve its performance, treated as a black-box under the function defined above, and the optimization handler, operating the black-box simulation and gradually improves the performance of the design variables over time.

For the first part, the orbital simulation, we used a number of Python scripts to handle the constellation analysis and interface with the Orekit [35] astrodynamics library to perform the computationally expensive operations such as orbital propagation and DoP calculation. The scripts take an input of the seven input variables and return the output performance metrics of the given constellation. For the latter part, the optimization handler, Python was again used to handle the optimization, queue the set of constellations being analyzed, and parallelize them over the CPU cores on the machine used. To perform the optimization, the Pymoo [36] library was used which has a range of functions to assist with defining the optimization problem and implements the desired multi-objective optimization (MOO) algorithm. We will be using the C-TAEA algorithm proposed by Li et al. [37], whose design aims to drive the population towards the Pareto front while simultaneously preserving diversity within the design space. C-TAEA is a state-of-the art multi-objective optimization algorithm which improves upon previous MOO algorithms such as NSGA-III [38] and Borg-MOEA [39] to allow for constraints applied to each of the objectives, allowing for faster convergence if the range of feasible solution is already known or defined – e.g. the maximum number of satellites allowable in the constellation design.

A summary of this setup can be seen in Fig. 2, illustrating the interfaces between each software used and the actions each take in carrying out the methodology. The methodology has been used in the past by studies aiming to optimize the design of Earth-based satellite constellations [40–42], as well as by Pereira et al. in the optimization of Lunar GNSS constellations [12].

4.1. Detailed software setup

4.1.1. Multi-objective optimization

The goal of using this approach is to take a representative set of initial constellation designs and to gradually improve them using a genetic approach to arrive at the Pareto front of non-dominated optimal

Table 5
Bounds of the input variables.

Variable	Type	Lower	Upper
a	Real	5000.0	50,000.0
e	Real	0.0	0.5
i	Real	0.0	90.0
ω	Real	0.0	360.0
s	Integer	3	10
p	Integer	3	10
f	Real	0.0	1.0

solutions. This is where no objective value can be improved further without harming the performance of another objective.

Within Pymoo [36], the function is defined as a seven variable, four objective problem. The bounds of the input variables are shown in Table 5.

The constraints placed on the objectives are shown in Eqs. (3) (4) (5) (6). The value of f is not the actual phase offset used in the simulation and is instead calculated as shown in Eq. (7), due to how the maximum phase offset is the number of orbital planes minus one — changing from constellation to constellation.

$$PDoP \leq 10.0 \tag{3}$$

$$HDoP \leq 10.0 \tag{4}$$

$$s \cdot p \tag{5}$$

$$\Delta V \leq 1.0 \tag{6}$$

$$\text{phase offset} = f(p - 1) \tag{7}$$

The optimization process has a population size of 200 constellation designs and the initial set of designs were selected using the Riesz s-Energy [43] method to define a set of reference directions creating a representative initial population, covering the whole design space. This minimizes the risk of the algorithm not finding the global minimum or converging on a non-global minimum. In the study C-TAEA has been configured using a Simulated Binary Crossover [38] with a probability of 0.75 and eta of 5.0, and a Polynomial Mutation with an eta of 10.0

4.2. Constellation analysis

Working underneath the MOO algorithm are the scripts which simulate and analyze the performance of each constellation design generated during the optimization process.

We use a combination of Python scripts interfacing with the Orekit Astrodynamics library [35], to perform the orbital propagation of each satellite, as well as calculate the DoP values and station-keeping ΔV.
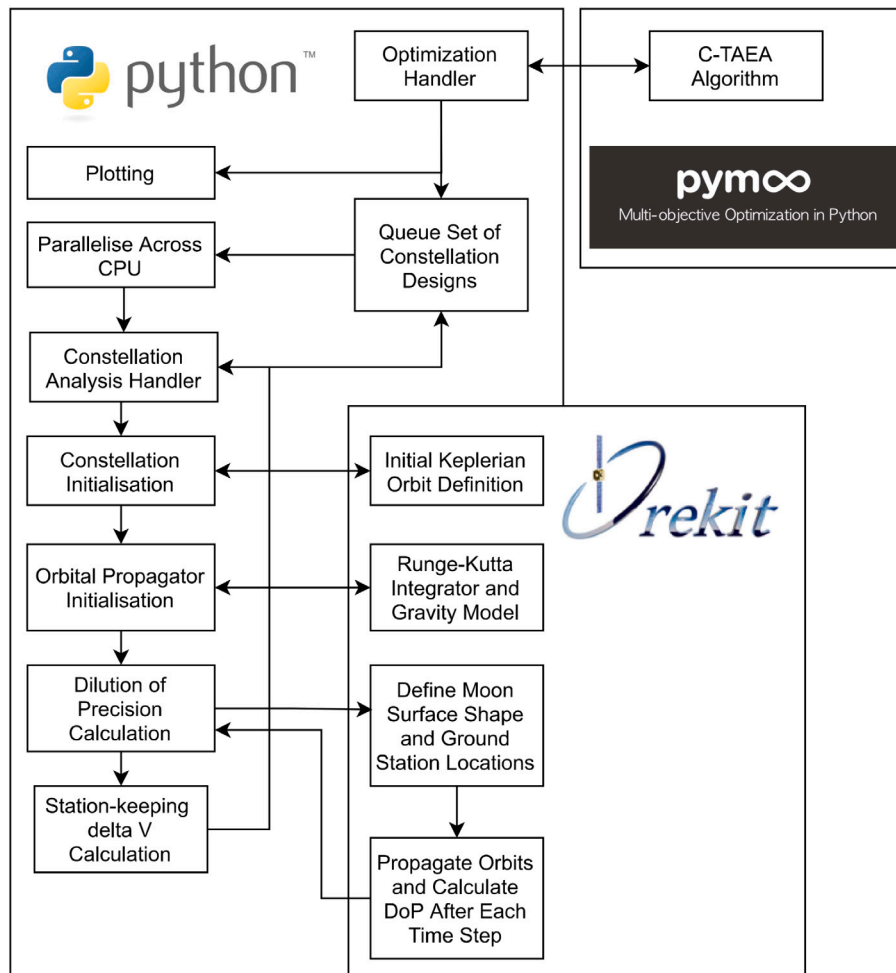
Fig. 2. Systems diagram showing software setup and the interface between each of the main software libraries used.

This setup was chosen because, although Python is a slow language, compared to compiled languages, Orekit is written and compiled in Java, allowing the majority of the computationally intensive work to be performed in an efficient language.

First, the individual constellation design is input from the optimization script to the analysis script. This includes the semi-major axis, eccentricity, and orbital inclination of each satellite, the number of orbital planes, number of satellites per plane, and the phase offset. From these values, the script defines the initial orbit and position of each satellite within the constellation around the Moon. This is done by creating a Keplerian Orbit [44] object within the Orekit Python wrapper [45].

Second, the script initializes a Numerical Propagator object for each of these satellites using the Orekit Python wrapper. The propagator uses the classical 4th Order Runge Kutta numerical integrator [46]and creates a gravity model which includes: a 10, 10 Holmes Featherstone [47] attraction model of the Moon, the Earth and Sun modeled as Third Body attractions [48], and a Solar Radiation Pressure attraction model [49] with a surface area of 3.92 m^2 and a reflection coefficient of 1.8. Each satellite is assumed to have a mass of 250 kg — approximately that of a SpaceX Starlink satellite [50].

Third, the surface of the Moon is defined as a Fibonacci sphere [51] of 500 points, representing the location of a GNSS receiver at each point on the surface. Using the Orekit Python wrapper, DoP Computer [52] objects are defined at each of these points with a minimum elevation value of 10°.

Fourth, the orbit of each satellite is propagated in steps of 900 s for a total of 14 days. After each time step, the PDoP & HDoP at each of the 500 points on the Lunar surface is calculated. If there are fewer than four satellites in view of a surface point, then the script returns a value of 1000.0 for both PDoP and HDoP.

Fifth, the station-keeping ΔV is calculated using the cost of a two maneuver Hohmann transfer and out-of-plane impulse burns [53]to return to the satellite's original semi-major axis, eccentricity, and inclination. This is a low precision analytical approach to reduce computation time and the values of ΔV should not be used as definite. The approach is appropriate in this case as a method to compare the relative cost of station-keeping maneuvers between designs.

Finally, the 3σ PDoP & HDoP for the constellation is calculated, using every data point calculated from all surface points, to represent the performance metric of the constellation. The mean station-keeping ΔV is calculated across each of the satellites within the constellation and these values are returned to the optimization script for further analysis.

5. Results and analysis

5.1. Data collected

After running the optimization script for 1864 generations, performing 372,800 constellation simulations, and generating 12,120 unique constellation designs (during the iteration process optimal designs are carried forward from one generation to the next), the Pareto front successfully converged.
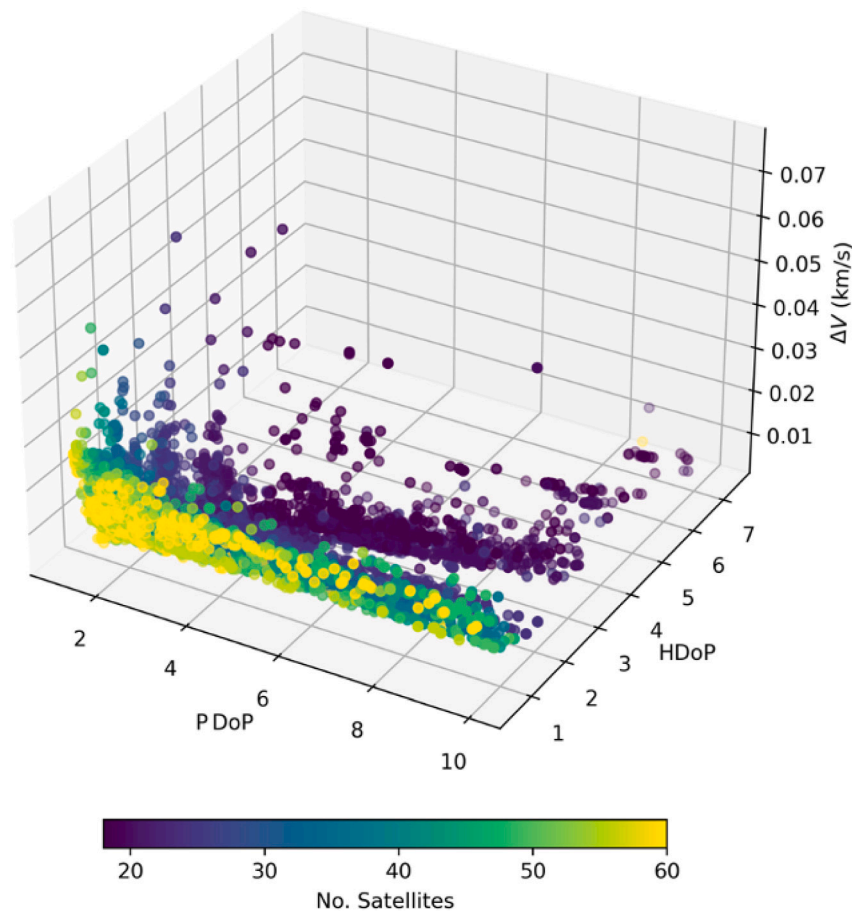
Fig. 3. Raw data set showing the performance of each constellation design. (For interpretation of the references to color in this figure legend, the reader is referred to the web version of this article.)

Fig. 3 compares the PDoP vs HDoP vs ΔV of the constellations considered with the number of satellites within the constellation indicated by the color, with a darker color indicating fewer satellites.

One can clearly see the Pareto front formed in the bottom left corner of the plot, illustrating the boundary of best performance available within the limits placed on the design variables. In the raw data, constellations with a greater number of satellites dominate the Pareto front – as one would intuitively expect – due to the greater number of satellites available, on average, at any one time to perform PNT calculation with.

However, as we are also trying to minimize the number of satellites in each constellation, this does not give us a complete picture of which designs are the most optimal. To do this a decomposition of the results must be performed to obtain an overall weighted 'cost' of each design.

5.2. Results

After the results of the performance metrics – PDoP, HDoP, ΔV, T – were collected from the optimization process, the individual values of each metric were scaled relative to the min/max of each. From this a PBI decomposition [54] was performed on the scaled performance metrics with weightings shown in Eq. (8) to determine which constellation designs have the best balance of performance between each of the metrics. Designs with the minimum decomposition value have the 'best' overall performance.

$$[PDoP, HDoP, \Delta V, T] = [0.3, 0.3, 0.1, 0.3] \qquad (8)$$

A lower value was given to the weighting of the station-keeping ΔV because of the uncertainty in the method used to calculate it; the other three values can be calculated more accurately and reliability and have greater impact on the overall performance and cost.

The results of the decomposition can be seen in Fig. 4, showing a plot of PDoP vs HDoP vs Decomposition with the number of satellites per constellation again represented by the color.

As with Fig. 3, the constellations in Fig. 4 with the best PDoP/HDoP performance are those with the greatest number of satellites. However, those with the lowest decomposition value are those with a low PDoP and HDoP and a low number of satellites per constellation. A list of the 10 constellation designs with the lowest decomposition values can be found in Table 6.

These constellations are quite consistent in their design, compared to the overall design space available, with key variables ranging as follows:

- a: 19,138–27,813 km
- e: 0.0000–0.0430
- i: 56.07–68.45 degrees
- s: 3–8 satellites per plane
- p: 3–8 orbital planes
- T: 21–24 total satellites

Resulting in a range of performance of:

- PDoP: 2.60–3.29
- HDoP: 1.20–1.44
- ΔV: 0.0151–0.0329 km/s

Compared to the performance requirements set out in Table 4, all 10 of these designs can meet the performance requirements needed
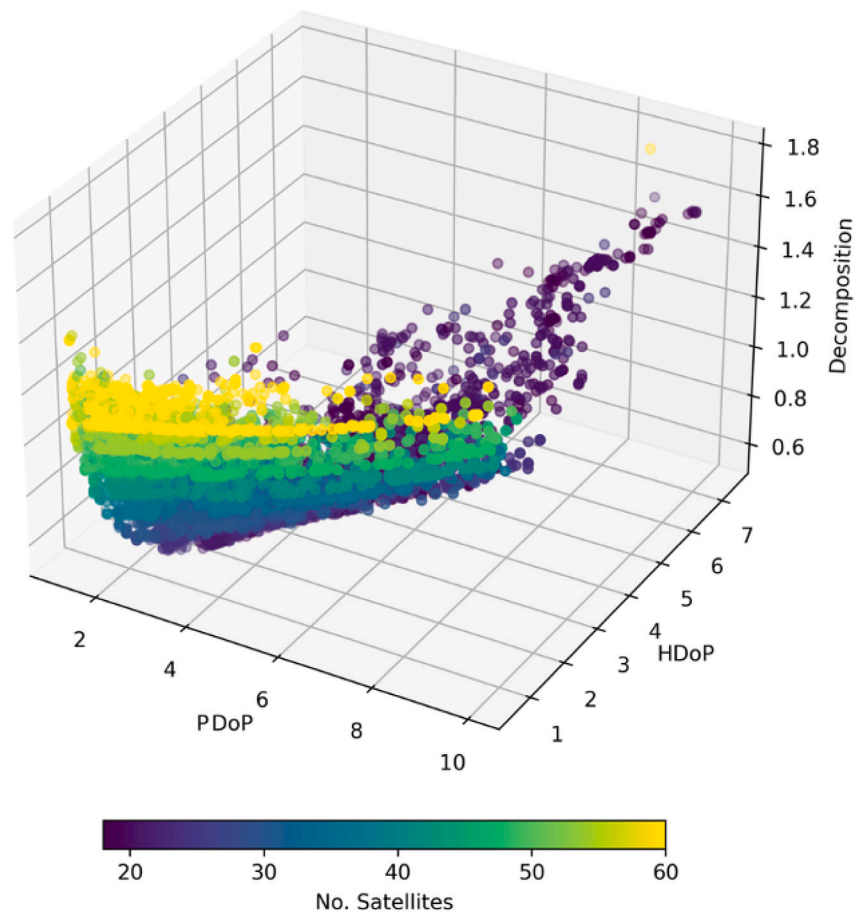
Fig. 4. The data set after decomposition to get a weighted overall performance of each design. (For interpretation of the references to color in this figure legend, the reader is referred to the web version of this article.)

Table 6
The design parameters and performance metrics of the 10 best designs obtained through the optimization process.

N	a	e	i	aop	s	p	f	$3\sigma PDoP$	$3\sigma HDoP$	ΔV (km/s)	T
1	24,572	0	58.69	22.90	4	6	0.2118	2.60	1.20	0.0266	24
2	24,531	0	58.69	22.90	4	6	0.3923	2.61	1.20	0.0265	24
3	26,652	0	67.38	298.14	4	6	0.3019	2.64	1.25	0.0262	24
4	24,589	0.0139	66.50	132.95	8	3	0.4641	2.62	1.30	0.0205	24
5	24,704	0.0065	68.45	134.34	8	3	0.4067	2.64	1.31	0.0220	24
6	27,211	0.0001	67.38	298.14	3	8	0.3019	2.71	1.23	0.0317	24
7	27,813	0.0001	64.37	298.14	3	8	0.3019	2.73	1.22	0.0329	24
8	19,148	0.0245	56.24	74.77	3	8	0.6778	2.75	1.16	0.0151	24
9	19,148	0.0245	56.07	74.77	3	8	0.6778	2.75	1.16	0.0151	24
10	22,352	0.0430	60.35	291.96	3	7	0.5864	3.29	1.44	0.0162	21

except for two operational modes. The modes which cannot be met are the Final Descent Phase when landing (0.4 PDoP) and the Moving Phase on the surface (0.1 HDoP). This is because these navigation requirements are not possible with the assumptions made of the UERE. These designs can therefore be considered as meeting feasible Lunar navigation requirements of future missions.

5.3. Comparison to literature

In comparison to the constellation designs proposed in the literature, having an average PDoP of 4.87 [12], the results shown here have an average PDoP of 2.73, representing a 44% decrease or improvement. No other paper has studied the HDoP performance, and the methodology used to calculate station-keeping ΔV is different so these values cannot be compared. In terms of the number of satellites used in the optimal constellations, our results and Pereira et al.'s [12] are similar (21 – 24 vs 20 – 24). This allows us to put the performance

improvement in perspective. The improvement has not been achieved through the use of more satellites in the constellation (increasing the cost), but instead due to the more efficient use of these satellites. Compared to the literature, these constellations use higher orbital altitudes and greater orbital inclinations allowing for greater coverage at the poles, demonstrating the limitation on performance imposed by Pereira et al.'s [12] to frozen orbit designs with an inclination of 40°.

Another comparison can be made against the studies performed in [6] with the use of 15 satellites distributed in different orbits as follow: 6x Elliptical Lunar Frozen Orbits (ELFO6) + 1x Near-Rectilinear Halo Orbits (NRHO1) + 4x Earth–Moon L2 Halo Orbit (L2 Halo4) + 4x Distant Retrograde Orbits (DRO4). This ELFO6 NRHO1 L2 Halo4 DRO4 arrangement produced 95% PDoP of 6.3, 4.5 and 11.7 on the Moon's far side on the equator with Lat./Lon.(0°/180°), Moon's far side with Lat./Lon. (−60°/180°), and the Moon's South Pole with Lat./Lon. (−90°/0°) respectively.

6. Conclusion

In this paper we have studied the principles of GNSS and satellite constellation design, with the aim of optimizing the designing process of a GNSS constellation for the Moon. We have done this through the numerical simulation, using Orekit, of a wide range of constellation designs, optimized iteratively through the use of the C-TAEA multi-objective optimization algorithm.

We have built upon the work of Pereira et al. and Batista et al. by studying a wider range of constellation designs and by comparing the results against a set of navigation requirements proposed by ESA. As a result, we have produced a range of constellation designs which, on average, achieve a 44% improvement relative to the designs proposed by Pereira et al. using the same number of satellites per constellation. These designs can also meet feasible navigation requirements set out by ESA .

The reason for this improvement, compared to the designs in the literature, is the increased range in designs considered. Pereira et al.'s study was limited to frozen orbit conditions with orbital altitudes below 17,370 km and inclinations of 40°. The results, however, all have an orbital altitude and inclination above these limits. The greater orbital altitude allows each satellite to cover more of the surface at any one time and the greater inclination allows the satellites to cover more of the surface at the poles compared to a lower inclination. Out of the 10 designs proposed in Table 6, the overall optimal design is constellation 4. This is because they have the fewest number of orbital planes out of the optimal designs, minimizing cost. Compared to the constellation with optimal decomposition value (1), the design has a PDoP difference of 0.7% and HDoP of 8% with the same number of satellites and a reduction in planes by 3.

6.1. Future work

One limitation of this study is the methodology chosen to calculate the station-keeping ΔV. The analytical approach used was chosen to reduce the computational load on the optimization process and allow us to prioritize on studying the PDoP and HDoP performance of each constellation. To improve the reliability of these results, a simulation approach should be taken, finding the actual orbital maneuvers required and propagating this forward to calculate the necessary ΔV.

However, this would require greater computational complexity and would necessitate a more confined study of fewer constellation designs — now possible due to the results in this paper. Future research should consider the constellation designs in Table 6 highlighting a baseline for any study on the optimization and implementation of a Lunar GNSS.

Declaration of competing interest

The authors declare that they have no known competing financial interests or personal relationships that could have appeared to influence the work reported in this paper.

Acknowledgments

References

[1] ISECG, Global Exploration Roadmap Critical Technology Needs-2019, International Space Exploration Coordination Group (ISECG), 2019, pp. 1–67, URL https://www.globalspaceexploration.org/wp-content/uploads/2019/12/2019_GER_Technologies_Portfolio_ver.IR-2019.12.13.pdf.

[2] L. Xiao, Farside Landing and Nearside Sample Return. China's New Lunar Missions Are on the Way, The Planetary Report, 2018, pp. 13–16, URL https://www.planetary.org/articles/china-new-lunar-missions.

[3] NASA, NASA's Lunar Exploration Program Overview, National Aeronautics and Space Administration, Headquarters Washington, DC, 2020, URL https://www.nasa.gov/sites/default/files/atoms/files/artemis_plan-20200921.pdf.

[4] ISECG, The Global Exploration Roadmap January 2018, International Space Exploration Coordination Group (ISECG), 2018, URL https://www.nasa.gov/sites/default/files/atoms/files/ger_2018_small_mobile.pdf.

[5] G.B. Palmerini, M. Sabatini, G. Perrotta, En route to the Moon using GNSS signals, Acta Astronaut. 64 (2009) 467–483, http://dx.doi.org/10.1016/j.actaastro.2008.07.022.

[6] A. Delépaut, M. Schönfeldt, P. Giordano, D. Blonski, R. Sarnadas, L. Ries, J. Ventura-Traveset, A system study for cislunar radio navigation leveraging the use of realistic Galileo and GPS signals, in: 32nd International Technical Meeting of the Satellite Division of the Institute of Navigation, ION GNSS+ 2019, Miami, Florida, 2019, pp. 1199–1219.

[7] A. Delépaut, P. Giordano, J. Ventura-Traveset, D. Blonski, M. Schönfeldt, P. Schoonejans, S. Aziz, R. Walker, Use of GNSS for lunar missions and plans for lunar in-orbit development, Adv. Space Res. 66 (2020) 2739–2756, http://dx.doi.org/10.1016/j.asr.2020.05.018.

[8] V. Capuano, C. Botteron, J. Leclère, J. Tian, Y. Wang, P.-A. Farine, Feasibility study of GNSS as navigation system to reach the Moon, Acta Astronaut. 116 (2015) 186–201, http://dx.doi.org/10.1016/j.actaastro.2015.06.007.

[9] N. Witternigg, G. Obertaxer, M. Schönhuber, J. Research, G.B. Palmerini, F. Rodriguez, L. Capponi, F. Soualle, J.-J. Floch, Weak GNSS signal navigation for lunar exploration missions, in: Proceedings of the 28th International Technical Meeting of the Satellite Division of the Institute of Navigation, ION GNSS+ 2015, Tampa, Florida, USA, 2015, pp. 3928–3944, URL https://www.researchgate.net/publication/303842754_Weak_GNSS_Signal_Navigation_for_Lunar_Exploration_Missions.

[10] ESA, Earth-moon navigation / system study and development of a highly-sensitive spaceborne receiver prototype, 2020, URL https://navisp.esa.int/project/details/88/show.

[11] A. Batista, E. Gomez, H. Qiao, K. Schubert, Constellation design of a lunar global positioning system using CubeSats and chip-scale atomic clocks, in: H.R. Arabnia, L. Deligiannidis, A. Solo (Eds.), Conference: WorldComp 2012 Proceedings - Embedded Systems and Applications, ESA, Las Vegas, Nevada, USA, 2012.

[12] F. Pereira, D. Selva, Exploring the design space of lunar GNSS in frozen orbit conditions, in: 2020 IEEE/ION Position, Location and Navigation Symposium, PLANS, 2020, pp. 444–451, http://dx.doi.org/10.1109/PLANS46316.2020.9110202.

[13] C. Hegarty, E. Kaplan, Understanding GPS Principles and Applications, second ed., 2005.

[14] J.G. Walker, Satellite constellations, J. Br. Interplanet. Soc. 37 (1984) 559.

[15] L. Rider, Analytic design of satellite constellations for zonal earth coverage using inclined circular orbits, J. Astronaut. Sci. 34 (1986) 31–64.

[16] D.C. Beste, Design of satellite constellations for optimal continuous coverage, IEEE Trans. Aerosp. Electron. Syst. AES-14 (1978) 466–473, http://dx.doi.org/10.1109/TAES.1978.308608.

[17] P. Groves, Principles of GNSS, Inertial, and Multisensor Integrated Navigation Systems, Second Edition, 2013.

[18] R.M. Smith, N. Merancy, J. Krezel, Exploration missions 1, 2, and beyond: First steps toward a sustainable human presence at the moon, in: 2019 IEEE Aerospace Conference, 2019, pp. 1–12, http://dx.doi.org/10.1109/AERO.2019.8742118.

[19] R.M. Smith, M. Gates, A. Cassady, J. Krezel, An overview of NASA's exploration mission 2 (EM-2), in: 2018 IEEE Aerospace Conference, 2018, pp. 1–11, http://dx.doi.org/10.1109/AERO.2018.8396585.

[20] NASA, NASA's first flight with crew important step on long-term return to the moon, missions to mars, 2019, URL https://www.nasa.gov/feature/nasa-s-first-flight-with-crew-important-step-on-long-term-return-to-the-moon-missions-to.

[21] V.D. Tana, B. Cotugno, S. Simonetti, G. Mascetti, E. Scorzafava, S. Pirrotta, ArgoMoon: There is a nano-eyewitness on the SLS, IEEE Aerosp. Electron. Syst. Mag. 34 (2019) 30–36, http://dx.doi.org/10.1109/MAES.2019.2911138.

[22] J. Marshall, Press release: Intuitive machines unveils 2021 moon landing navigation approach, 2020, URL https://www.intuitivemachines.com/post/intuitive-machines-unveils-2021-moon-landing-navigation-approach.

[23] G. Ju, J. BAE, S. jin CHOI, W.B. LEE, C.J. LEE, New Korean lunar exploration program (KLEP): an introduction to the objectives, approach, architecture, and analytical results, in: 64th International Astronautical Congress Proceedings. Beijing, China, Beijing, China, 2013.

[24] Y.-R. Kim, Y.-J. Song, Observational arc-length effect on orbit determination for Korea pathfinder lunar orbiter in the earth-moon transfer phase using a sequential estimation, J. Astron. Space Sci. 36 (2019) 293–306, http://dx.doi.org/10.5140/JASS.2019.36.4.293.

["